

February 1, 2008

GRB 070610: A Curious Galactic Transient

*M. M. Kasliwal¹, S. B. Cenko², S. R. Kulkarni¹, P. B. Cameron¹, E. Nakar¹, E. O. Ofek¹,
 A. Rau¹, A. M. Soderberg¹, S. Campana³, J. S. Bloom⁴, D. A. Perley⁴, L. K. Pollack¹⁷,
 S. Barthelmy⁵, J. Cummings⁵, N. Gehrels⁵, H. A. Krimm^{6,16}, C. B. Markwardt^{6,7},
 G. Sato⁵, P. Chandra⁸, D. Frail⁹, D. B. Fox¹⁰, P. Price¹¹, E. Berger^{12,13}, S. A. Grebenev¹⁴,
 R. A. Krivonos^{14,15} & R. A. Sunyaev^{14,15}*

ABSTRACT

GRB 070610 is a typical high-energy event with a duration of 5 s. Yet within the burst localization we detect a highly unusual X-ray and optical transient,

¹Division of Physics, Mathematics and Astronomy, California Institute of Technology, MS 105-24, Pasadena, CA 91125, USA

²Space Radiation Laboratory, California Institute of Technology, MS 220-47, Pasadena, CA 91125, USA

³INAF, Osservatorio Astronomica di Brera, via E. Bianchi 46, I-23807 Merate (LC), Italy

⁴Department of Astronomy, University of California, Berkeley, CA 94720, USA

⁵NASA Goddard Space Flight Center, Greenbelt, MD 20771, USA

⁶CRESST and Astroparticle Physics Laboratory, NASA/GSFC, Greenbelt, MD 20771, USA

⁷Department of Astronomy, University of Maryland, College Park, MD 20742, USA

⁸University of Virginia, P.O. Box 400325, Charlottesville, VA 22903, USA

⁹National Radio Astronomy Observatory, Socorro, NM 87801, USA

¹⁰Department of Astronomy & Astrophysics, 525 Davey Laboratory, Pennsylvania State University, University Park, PA 16802, USA

¹¹Institute for Astronomy, University of Hawaii, 2680 Woodlawn Drive, Honolulu, HI 96822, USA

¹²Observatories of the Carnegie Institute of Washington, Pasadena, CA 91101, USA

¹³Princeton University Observatory, Princeton, NJ 08544, USA

¹⁴Space Research Institute, Profsoyuznaya 84/32, 117997 Moscow, Russia

¹⁵Max-Planck-Institut fuer Astrophysik, Karl-Schwarzschild-Str. 1, D-85741 Garching, Germany

¹⁶Universities Space Research Association, 10211 Wincopin Circle, Suite 500, Columbia, MD 21044

¹⁷Department of Astronomy and Astrophysics, University of California, Santa Cruz, CA 95064

Swift J195509.6+261406. We see high amplitude X-ray and optical variability on very short time scales even at late times. Using near-infrared imaging assisted by a laser guide star and adaptive optics, we identified the counterpart of *Swift* J195509.6+261406. Late-time optical and near-infrared imaging constrain the spectral type of the counterpart to be fainter than a K-dwarf assuming it is of Galactic origin. It is possible that GRB 070610 and *Swift* J195509.6+261406 are unrelated sources. However, the absence of a typical X-ray afterglow from GRB 070610 in conjunction with the spatial and temporal coincidence of the two motivate us to suggest that the sources are related. The closest (imperfect) analog to *Swift* J195509.6+261406 is V4641 Sgr, an unusual black hole binary. We suggest that *Swift* J195509.6+261406 along with V4641 Sgr define a sub-class of stellar black hole binaries – the fast X-ray novae. We further suggest that fast X-ray novae are associated with bursts of gamma-rays. If so, GRB 070610 defines a new class of celestial gamma-ray bursts and these bursts dominate the long-duration GRB demographics.

Subject headings: *gamma rays:bursts* – *X-rays:bursts* – *X-rays: individual (Swift J195509.6+261406)* – *stars:flare* – *X-rays: binaries*

Facilities: PO:1.5m, Hale, Keck:I, Keck:II, VLA, Swift

1. Discovery of GRB 070610

Launched in November 2004, the *Swift* Gamma-Ray Burst Explorer (Gehrels et al. 2004) was designed to localize γ -ray bursts (GRBs) and undertake rapid and sustained X-ray and Ultra-Violet observations of the resulting afterglow. With over two hundred events now localized and studied, *Swift* has made fundamental contributions to both long-duration soft bursts (LSBs) and short-duration hard bursts (SHBs). LSBs appear to trace cosmological massive-star formation rate with one event at a redshift of 6.3. SHBs have been seen at typical redshifts of ~ 0.5 in both elliptical and star-forming galaxies. There is now some circumstantial evidence for SHBs being the result of coalescence of compact objects.

At 20:52:26 UT on 2007 June 10 the Burst Alert Telescope (BAT; Barthelmy et al. 2005) aboard *Swift* triggered on GRB 070610. The high-energy prompt emission had a duration (T_{90}) of 4.6 s (Pagani et al. 2007a). Over the range 15–150 keV the burst could be fitted with a power law with photon index $\Gamma = 1.76 \pm 0.25$, resulting in a fluence of $(2.4 \pm 0.4) \times 10^{-7}$ erg cm $^{-2}$ (Tueller et al. 2007). A blackbody model is inconsistent with this emission (reduced $\chi^2 = 1.7$).

The burst profile consisted of a single symmetric peak (Figure 1). Fitting the profile (Norris et al. 1996), we calculate a rise time (i.e. half width at half maximum) of 1.68 ± 0.55 s. As can be seen from Figure 2, the duration and the hardness ratio of *Swift* J195509.6+261406 are both consistent with the broader population of extragalactic long-duration GRBs observed by *Swift*.

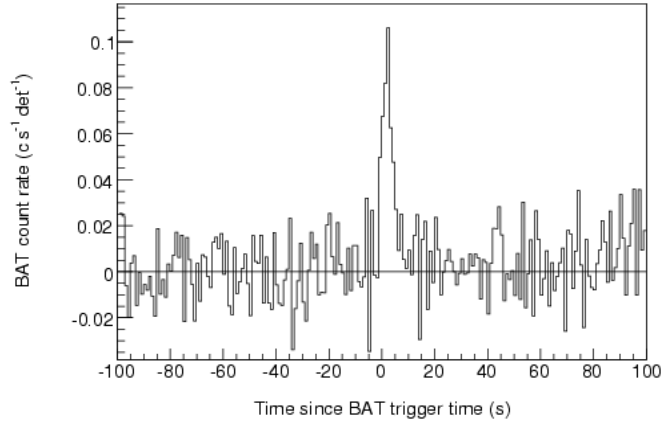


Fig. 1.— 15-150 keV *Swift*-BAT light curve of GRB 070610, with 1-s time resolution. The conversion factor to translate the ordinate to cgs flux units is $5.6 \times 10^{-7} \text{ erg cm}^{-2} \text{ c}^{-1} \text{ det}$ (1 det = 0.16 cm²).

The BAT localized GRB 070610 to $\alpha = 19^{\text{h}}55^{\text{m}}13''.1$, $\delta = +26^{\circ}15'20''$ (J2000.0) and a 90%-containment radius of $1.8'$. As can be seen in Figure 3 the field is dense, which is not surprising given the Galactic location ($l = 63.3^{\circ}$ and $b = -1.0^{\circ}$).

Here we report the discovery of an unusual X-ray transient (hereafter referred to as *Swift* J195509.6+261406) in the error circle of GRB 070610 and followup optical, near-infrared (NIR) and radio observations.

2. *Swift* J195509.6+261406: A Transient X-ray Source

The X-ray Telescope (XRT; Burrows et al. 2005) began observing the field of GRB 070610 3.2 ks after the initial BAT trigger (prompt slewing was disabled due to an Earth limb constraint). The XRT detected a single uncatalogued variable source in the BAT error circle at $\alpha = 19^{\text{h}}55^{\text{m}}9''.6$, $\delta = +26^{\circ}14'6''.7$ (90% confidence error circle of $4''.3$ radius; Pagani et al. 2007b). This position was further refined to $\alpha = 19^{\text{h}}55^{\text{m}}9''.66$, $\delta = +26^{\circ}14'5''.2$ (90% confi-

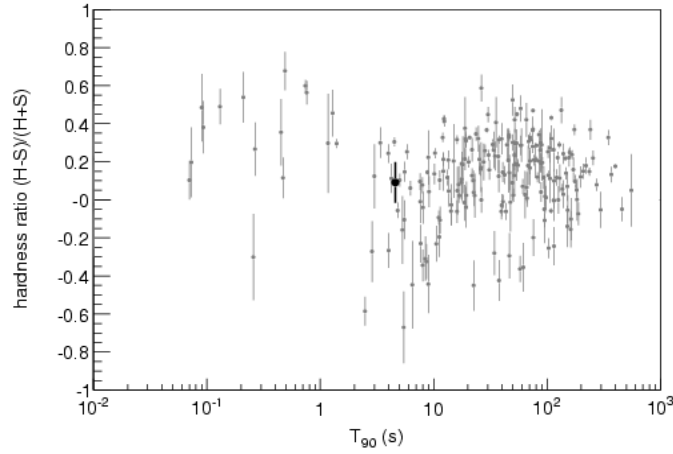


Fig. 2.— Plot of duration (T_{90}) and hardness ratio (HR) of 226 *Swift* bursts from GRB 041217 to GRB 070616. We define hardness ratio as $(H - S)/(H + S)$, where S and H are energy fluences in 15–50 keV and 50–150 keV, respectively. The values of T_{90} and hardness ratio for GRB 070610 (marked by a large filled black circle) are 4.6 ± 0.4 s and 0.09 ± 0.11 (90% confidence level), respectively.

dence error circle of $1''.2$ radius ¹).

The XRT continued to monitor *Swift* J195509.6+261406 over the course of the next month until the source was no longer detected.

The XRT data were processed with `xrtpipeline` (v0.10.6). All data were obtained in photon counting mode. In this mode the entire CCD is read and the time resolution is limited to 2.5 s. We extracted grade 0–12 events (Burrows et al. 2005) from a 15 pixel radius circular region centered on the source. To account for the background, we extracted events within a 40 pixel radius circular region in the vicinity of the transient but not encompassing any other source in the field. We adaptively extracted the light curve binning the data in order to have 10 counts per bin. The light curve was corrected for the extraction region losses and for CCD defects as well as for vignetting by using the task `xrtlccorr` (v0.1.9), which generates an orbit-by-orbit correction based on the instrument map.

The X-ray light curve of *Swift* J195509.6+261406 is shown in Figure 4 and compared to a small sample of long-duration GRB afterglows in Figure 5. Kann et al. 2007 were the first to suggest that this GRB was likely to be of Galactic origin. Clearly, *Swift* J195509.6+261406

¹http://astro.berkeley.edu/~nat/swift/xrt_pos.html

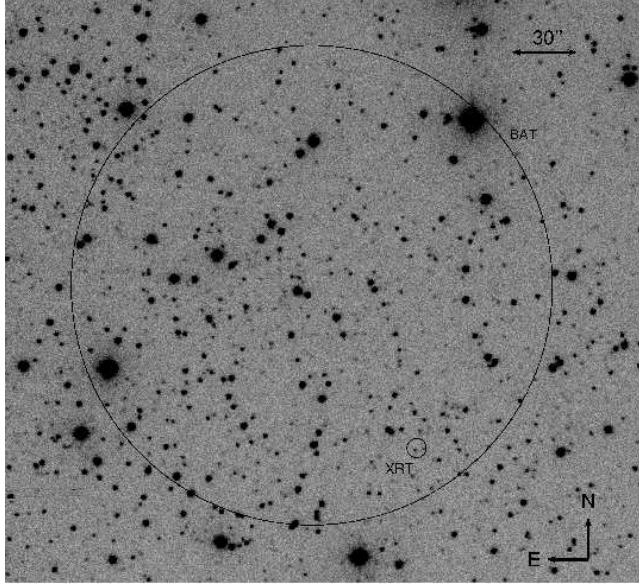


Fig. 3.— Optical image (i' -band) of the field of GRB 070610 obtained by the automated Palomar 60-inch telescope on UT 2007 June 12. The BAT localization of GRB 070610 has a radius of $1.8'$, while the XRT localization of *Swift* J195509.6+261406 has a radius of $4.3''$; both are indicated with black circles. The bright source in the XRT circle is *Swift* J195509.6+261406 .

differs from typical GRB X-ray afterglows in two fundamental respects. First, it does not exhibit the strong (overall) secular decrease in flux over timescales of hours (Nousek et al. 2006; Zhang et al. 2006). While the decay index in long-duration GRBs can vary markedly from one phase to another, *Swift* J195509.6+261406 shows no significant decline until very late times ($\sim 10^6$ s).

Secondly, the XRT light curve of *Swift* J195509.6+261406 consists of spikes – never seen before in any afterglow. In particular we draw the attention of the reader to a dramatic flare at $t \sim 7.86 \times 10^4$ s, jumping by a factor of $\Delta f/f \sim 100$ in flux over a time scale of $\Delta t/t \sim 10^{-4}$ (see Figure 4, inset). None of the sixty nine XRT flares described in Chincarini et al. (2007) exhibit a comparable amplitude spike at late time. While a strong X-ray flare has been seen in GRB 050502B (Falcone et al. 2006) (see Figure 5) the fractional duration, $\Delta t/t$ is much larger (~ 0.5). Less significant variability is present throughout the duration of observations of *Swift* J195509.6+261406 .

We searched the XRT flare for pulsations. 521 photons were extracted withing $60''$ of the source position and corrected to the solar system barycenter with the task `barycorr`. To search for pulsations we constructed the Z_1^2 power spectrum to a maximum frequency of 0.2 Hz (Bucccheri et al. 1983). The largest observed value of Z_1^2 was 25.2 at a frequency of

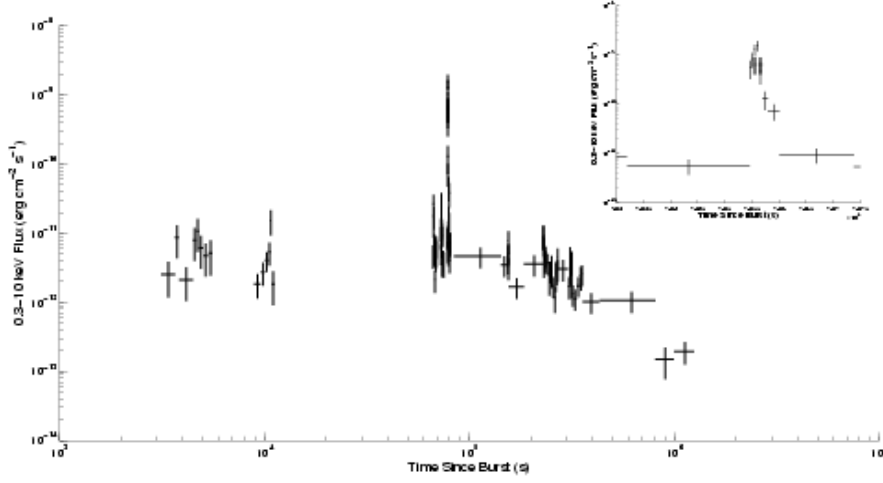


Fig. 4.— XRT light curve of *Swift* J195509.6+261406 in the energy band 0.3–10 keV. The dramatic X-ray flare at $t \sim 7.86 \times 10^4$ s is shown in the inset.

0.1446 Hz. Since Z_n^2 is distributed as χ^2 with $2n$ degrees of freedom, this value corresponds to a single trial detection significance of 4.8σ in equivalent Gaussian units. Given that we have performed 350 trials, the significance of this detection is 3.4σ , and thus we do not consider this result to be conclusive evidence of periodicity.

For spectral analysis the ancillary response files were generated with the task `xrtmkarf`. We used the latest spectral redistribution matrices (v009). Data were extracted from single or consecutive orbits in order to have at least 100 counts per spectrum. Spectra were binned to a minimum of 15 counts per energy bin. The resulting spectra were inconsistent with a blackbody (reduced $\chi^2 = 1.9$) and consistent with a power law model (task `phabs`). The best fit column density (N_H) and photon index (Γ) for each epoch are summarized in Table 1. Overall, we find that the inferred flux conversion is approximately 1 count $s^{-1} \approx 1.3 \times 10^{-10}$ erg cm^{-2} s^{-1} in the 0.3–10 keV band.

We extrapolate the XRT flare spectrum to BAT (15–50 keV) and predict a flux of 1.8×10^{-9} erg cm^{-2} s^{-1} . This corresponds to a BAT count rate of 0.0032 counts s^{-1} det^{-1} . This is consistent with a 2- σ upper limit from two 64s intervals of BAT data straddling the XRT flare — 0.0038 counts s^{-1} det^{-1} (at 78499.8s) and 0.012 counts s^{-1} det^{-1} (at 78563.8s).

The inferred interstellar extinction along this low Galactic latitude is quite high and thus uncertain: N_H of 1.1×10^{22} cm^{-2} (Dickey & Lockman 1990); 0.8×10^{22} cm^{-2} (Kalberla et al. 2005); and 1.56 – 1.89×10^{22} cm^{-2} (Schlegel et al. 1998). The former two estimates are based on H I data whereas the latter on diffuse infrared emission. Given the uncertainty in the inferred

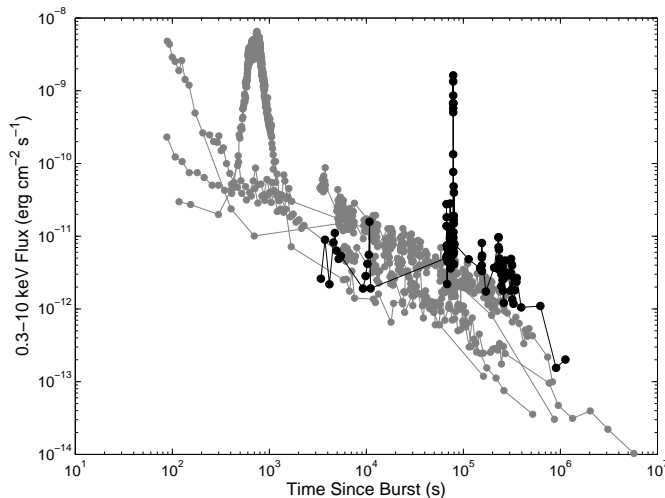


Fig. 5.— XRT light curves of a small sample of extragalactic long-duration GRBs (GRBs 050315, 050318, 050319, 050416A, and 050502B) are shown in grey. Data are from Evans et al. 2007. All show the approximately power-law decay typical of GRB afterglows. GRB 050502B exhibits a bright flare around $t \sim 10^3$ s (see Falcone et al. 2006). However, the rise time of this flare is much longer than the spike seen in *Swift* J195509.6+261406 (shown in black).

N_H the XRT spectrum cannot be used to determine the distance to *Swift* J195509.6+261406.

3. A Flickering Optical Variable

Rapid observations in response to the BAT trigger, in particular by the *OPTIMA-Burst* team (Stefanescu et al. 2007a), revealed a rapidly variable (time scales as low as tens of seconds) optical transient inside the XRT error circle of *Swift* J195509.6+261406. Astronomers using other facilities – including the OSN 1.5-m telescope (Postigo et al. 2007), the 2-m Schmidt telescope of the Thüringer Landessternwarte (Kann et al. 2007), the 25-cm *TAROT* facility (Klotz et al. 2007), and the 40-cm *Watcher* telescope (French et al. 2007) – confirmed the detection of this variable source. Detections and upper limits reported to the GRB Coordinates Network (GCN²) are shown in Figure 6.

Drawn by the excitement of these discoveries, we began monitoring the field of *Swift* J195509.6+261406 in the i' filter with the automated Palomar 60-inch telescope (P60; Cenko et al.

²http://gcn.gsfc.nasa.gov/gcn3_archive.html

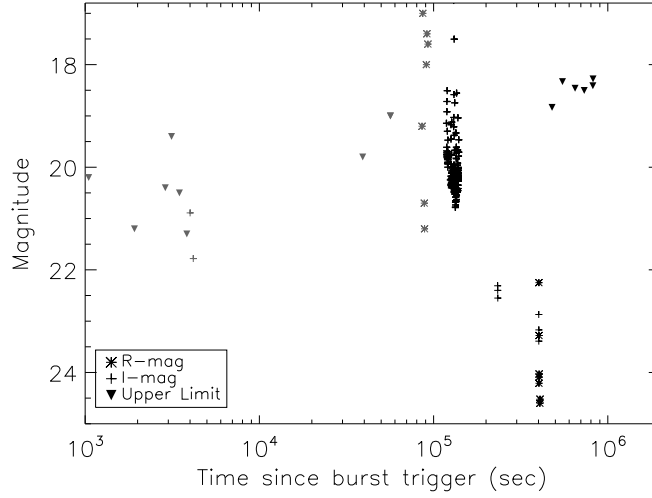


Fig. 6.— Optical light curve of *Swift* J195509.6+261406, including data from P60 (black), Keck/LRIS (black), and the literature (grey). (French et al. 2007; Postigo et al. 2007; Kann et al. 2007; Updike et al. 2007a; Stefanescu et al. 2007b; Yoshida et al. 2007; Klotz et al. 2007; Stefanescu et al. 2007c; Updike et al. 2007b).

2006) starting at 5:47 UT 2007 June 12 and continued over the next several nights. In addition, we imaged the field in *R*-, *I*- and *g*- bands with the *Low Resolution Imaging Spectrograph* (LRIS; Oke et al. 1995) mounted at the Cassegrain focus of the Keck I 10-m telescope. All images were reduced using standard IRAF³ routines.

The light curve obtained from our observations is also summarized in Figure 6. The P60 and the Keck photometry can be found in Table 5 and Table 2 respectively.

The P60 light curve is dominated by flickering and magnificent flares on the night of UT 2007 June 12 (see Figure 7). We observed over eleven flares with amplitudes greater than one magnitude in only three hours. The brightest of these flares rose and dropped by more than 3.5 magnitudes within 6 minutes. The amplitude of the flares is a lower limit because the P60 images are not deep enough to detect the quiescent counterpart (see below). The timescale is also an upper limit because it is entirely possible that variability is more rapid than our sampling rate (~ 60 s). If we define duty-cycle as the fraction of time for which the *Swift* J195509.6+261406 was brighter than $i' < 20$, then the duty cycle based on the first night of data is 18.6%. Given that there was no detection on subsequent ten nights, the

³IRAF is distributed by the National Optical Astronomy Observatory, which is operated by the Association for Research in Astronomy, Inc., under cooperative agreement with the National Science Foundation.

Table 1. XRT Spectral Analysis

Epoch Start (MJD)	Total Exposure (s)	N_{H} (10^{22} cm^{-2})	Γ
54261.907	4811	$0.30^{+0.29}_{-0.23}$	1.43 ± 0.37
54262.641	7912	$0.76^{+0.24}_{-0.18}$	1.93 ± 0.18
54263.268, 54264.004	2947, 10500	$0.59^{+0.31}_{-0.23}$	1.11 ± 0.22
54265.387	6026	$0.61^{+0.53}_{-0.33}$	1.33 ± 0.40
Flare	...	$0.92^{+0.91}_{-0.57}$	1.74 ± 0.48
All but flare	...	$0.72^{+0.14}_{-0.12}$	1.71 ± 0.11

Note. — We have fit the XRT data to a power-law model of the form $N(E) \propto E^{-\Gamma}$, leaving the line-of-sight N_{H} as a free parameter.

Table 2. Optical Observations of *Swift* J195509.6+261406 at Keck I and Palomar Hale

Mean Epoch (2007 UT)	Facility	Filter	Exposure (s)	Magnitude (s)
Jun 13.570	LRIS	<i>I</i>	120×3	> 24.0
Jun 15.517	LRIS	<i>I</i>	200×3	24.37 ± 0.21
Jun 15.524	LRIS	<i>R</i>	180×1	22.25 ± 0.06
Jun 15.527	LRIS	<i>R</i>	180×1	24.21 ± 0.13
Jun 15.531	LRIS	<i>R</i>	180×1	23.28 ± 0.07
Jun 15.534	LRIS	<i>R</i>	180×1	24.09 ± 0.11
Jun 15.594	LRIS	<i>R</i>	45×8	> 25.0
Aug 13.336	LRIS	<i>R</i>	300×4	> 26.0
Sep 13.362	LFC	<i>i'</i>	360×26	> 24.5

Note. — Zeropoints computed in the Vega system. Error quoted are $1\text{-}\sigma$ photometric and instrumental errors summed in quadrature. Upper limits quote are $3\text{-}\sigma$. No correction has been made for the large line-of-sight extinction.

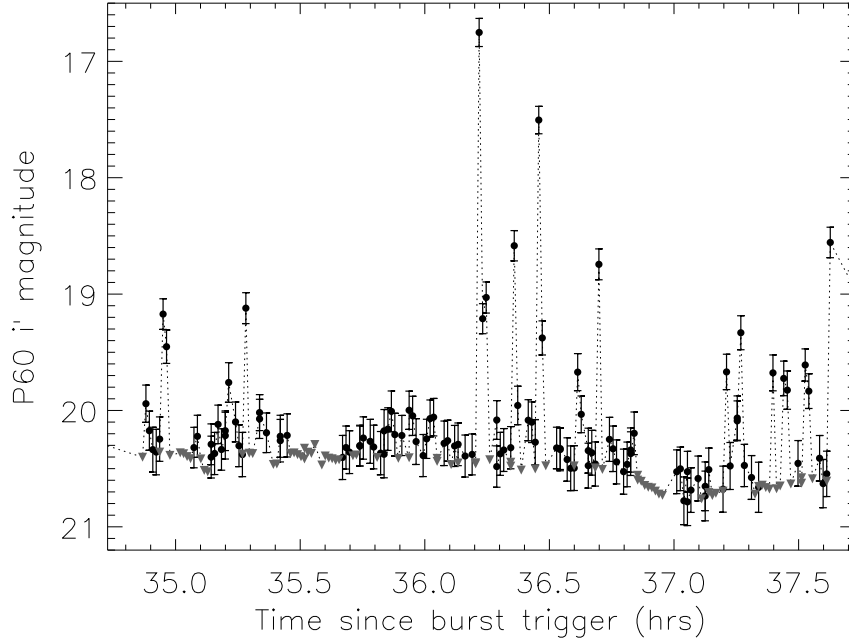


Fig. 7.— P60 i' -band light curve from the night of 2007 June 12. Upper limits are indicated by grey inverted triangles. The rapid variability (time scales less than 60 s, our sampling rate) at late times is unlike any previous long-duration GRB optical afterglow.

duty cycle reduces to 5.8%.

We see a dramatic flare in the *LRIS* data five days (UT 2007 June 15) after the high-energy emission, even though the peak magnitude is much fainter. The brightest observed flare in R -band was 2 magnitudes in three minutes (see Figure 8). Much like the behavior seen in X-rays (§2), such dramatic optical variability at late times is unlike anything seen before from an extragalactic GRB optical afterglow. Unfortunately none of our optical data directly overlap the XRT light curve, making a direct correlation between the two impossible.

Two months after the burst, the optical counterpart faded in R -band to fainter than 26.0 and three months after the burst, faded in i' -band to fainter than 24.5 (see Table 2).

4. A Near Infrared Counterpart

Given the large line-of-sight extinction, we undertook late-time NIR imaging at a variety of facilities to search for a quiescent counterpart to *Swift* J195509.6+261406. The results of

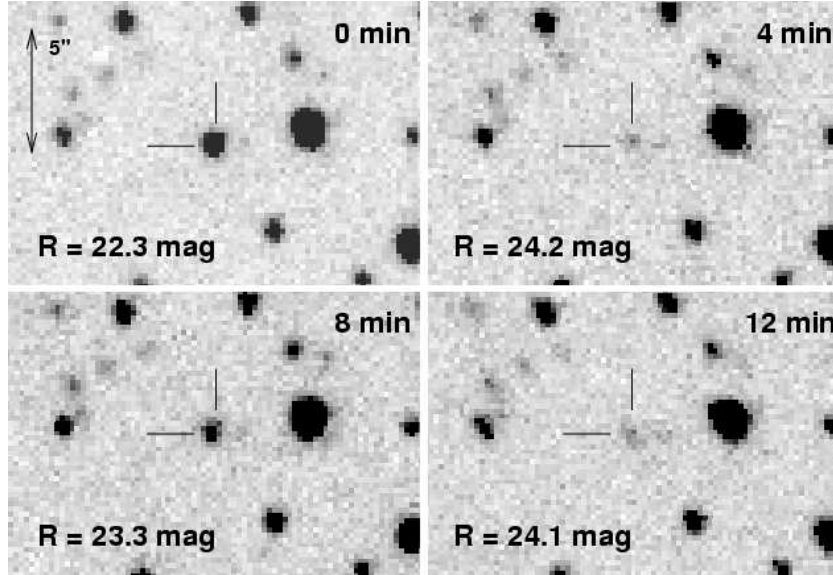


Fig. 8.— Close up view of the optical field of the *Swift* J195509.6+261406 optical transient using the *LRIS* instrument on the Keck I 10-m telescope; 2007 June 15 starting at 12:33 UT. All four images were taken in the *R*-band with a 180 s exposure in sequence. The transient brightens by over two magnitudes in only three minutes about five days after the burst trigger. Such rapid variability at late times is unprecedented from an extragalactic GRB optical afterglow.

our campaign are summarized in Table 3.

In detail, we observed the field of *Swift* J195509.6+261406 with the Near InfraRed Imager and spectrograph (NIRI; Hodapp et al. 2003) mounted on the 10-m Gemini North telescope on two occasions. On 2007 June 19 we obtained 18×60 s images in the *K*-band under exquisite seeing ($\sim 0.4''$) and photometric conditions. The observations on UT 2007 July 15 suffered from poor seeing and clouds.

On UT 2007 June 21, starting 13:10, we observed the transient with Laser Guide Star Adaptive Optics (LGS-AO; Wizinowich et al. 2006; van Dam et al. 2006) on the Keck II telescope and the Near-Infrared Camera 2 (NIRC2). A total of 17 images were obtained, each consisting of three 20 s co-added integrations, in the *K'* filter using the wide-angle camera. We also obtained further late-time observations on UT 2007 Sep 21 and UT 2007 Sep 30.

Finally, *J*- and *H*-band images were obtained with the Wide-Field Infrared Camera (WIRC; Wilson et al. 2003) mounted on the Palomar Hale 200-inch (P200) telescope. Thirty four images each with integration time of 30 s were taken in each filter on the night of UT 21 June 2007.

All but the LGS data were processed with standard IRAF routines. Custom routines in *Python* and *IDL* (written by JSB and LP) were used for the LGS-AO reductions; a custom distortion correction (obtained by PBC⁴) was applied to the LGS-AO imaging. We created an astrometric solution using our Gemini/NIRI *K*-band image from the night of June 19 relative to about fifty point sources from the 2- μ m All-Sky Survey (2MASS; Skrutskie et al. 2006). The resulting RMS positional uncertainty was $0.125''$ in right ascension and $0.098''$ in declination. This NIRI *K*-band image was then used to create a catalog of about one hundred point sources for astrometric matching with all other images. The NIRI *K*-band image was chosen because of the excellent seeing conditions ($\sim 0.4''$) and the larger field of view in comparison to NIRC2. Typical RMS positional uncertainties relative to the reference image were $\approx 0.07''$ in each coordinate. Using these astrometric solutions, we determine a position for the optical transient in the Keck *R*-band flares of $\alpha = 19^{\text{h}}55^{\text{m}}09^{\text{s}}.646$, $\delta = +26^{\circ}14'05''.62$ (J2000.0).

Despite the presence of two nearby objects (*A* and *B*), our astrometric accuracy is sufficient to unambiguously identify the *K*-band counterpart to *Swift* J195509.6+261406 (*X* in Figure 9). Using the LGS-AO/NIRC2 image, we find that the location of this NIR counterpart is $\alpha = 19^{\text{h}}55^{\text{m}}9^{\text{s}}.649$, $\delta = +26^{\circ}14'5''.65$ (J2000.0), with an uncertainty of 100 mas in each direction.

Due to the crowded field, PSF-matched photometry was performed on all images using the IRAF DAOPHOT package. We summarize our NIR observations in Table 3. For reference, the *RIJHK_s* magnitudes of two extremely nearby objects *A* and *B* are provided in Table 4. Our late-time data, over three and a half months after the burst, constrains the quiescent counterpart to be fainter than $K' > 21.5$.

5. Search for a radio counterpart

On 2007 June 15 we undertook Very Large Array (VLA)⁵ observations of *Swift* J195509.6+261406. The observations were obtained in 2×50 MHz bands around 8.46 GHz and lasted about an hour.

We observed 1956+283 (a phase calibrator) for 0.8 minutes and then switched to *Swift* J195509.6+261406 for 4.8 minutes. The sequence ended with a 6-minute observation of

⁴http://www2.keck.hawaii.edu/inst/n2TopLev/post_observing/dewarp/

⁵The National Radio Astronomy Observatory is a facility of the National Science Foundation operated under cooperative agreement by Associated Universities, Inc.

Table 3. NIR Observations of *Swift* J195509.6+261406

Epoch (2007 UT)	Facility	Filter	Magnitude
Jun 19.549	Gemini-N/NIRI	K	19.30 ± 0.23
Jun 21.220	Keck II/LGS-AO+NIRC2	K'	19.83 ± 0.15
Jul 15.309	Gemini-N/NIRI	K	> 19.5
Jun 21.352	P200/WIRC	J	> 20.5
Jun 21.400	P200/WIRC	H	> 19.5
Sep 21.632	Keck II/LGS-AO+NIRC2	K'	> 20.3
Sep 30.264	Keck II/LGS-AO+NIRC2	K'	> 21.5

Note. — Errors quoted are $1\text{-}\sigma$ photometric and instrumental errors summed in quadrature. Upper limits quoted are $3\text{-}\sigma$. No correction has been made for the large line-of-sight extinction.

Table 4. Photometry of Nearby Contaminating Sources *A* and *B*

Epoch (2007 UT)	Facility	Filter	Magnitude Source A	Magnitude Source B
Jun 15.594	Keck I/LRIS	R	> 25.0	> 25.0
Aug 13.336	Keck I/LRIS	R	> 26.0	> 26.0
Jun 15.517	Keck I/LRIS	I	24.83 ± 0.21	24.93 ± 0.22
Jun 21.352	P200/WIRC	J	> 20.5	> 20.5
Jun 21.400	P200/WIRC	H	> 19.5	> 19.5
Jun 21.220	Keck II/LGS	K'	20.30 ± 0.16	19.44 ± 0.14

Note. — Source B is 471 ± 22 mas West and 670 ± 22 mas South of *Swift* J195509.6+261406. In images with poorer angular resolution, stars A and B may contaminate the photometry of the transient (i.e. our NIRI imaging).

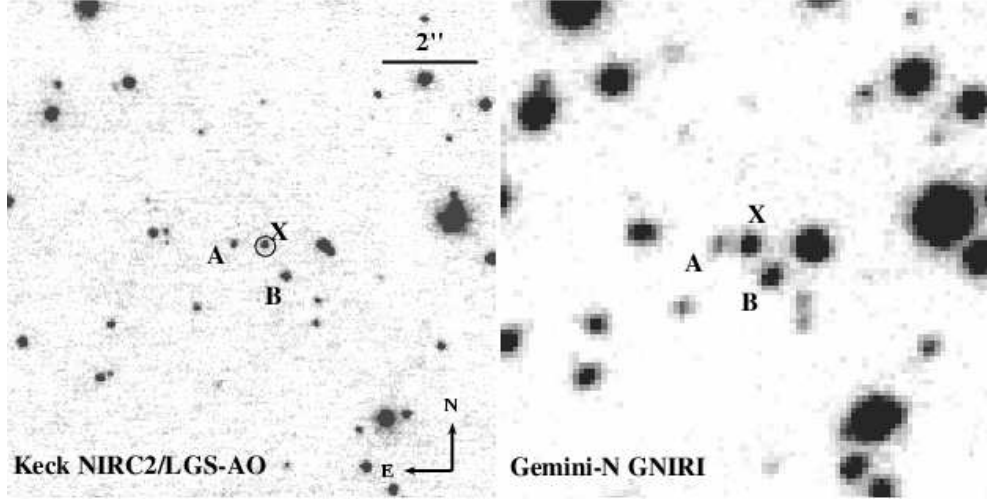


Fig. 9.— A K -band image of the field of *Swift* J195509.6+261406 obtained with NIRC-2 imager behind the Keck II Laser Guide Star (LGS) system (left; 2007 June 21) and NIRI imager on the Gemini-North telescope (right; 2007 June 19). The $2\text{-}\sigma$ error circle of the optical transient (taken from our *LRIS* imaging) is shown as a black circle overlaid on the LGS image. Clearly we can identify the object marked as 'X' as the NIR counterpart of *Swift* J195509.6+261406.

0137+331 (3C48; flux calibrator).

Data were analyzed using the Astronomical Image Processing System (AIPS) software of National Radio Astronomy Observatory (NRAO). VLA antennas N16, W64, E72 and W48 and baseline combinations EVLA antennas E16 W24, N64, W40, E56, W48 and N40 were flagged. In total, flagging resulted in a loss of about 100 baselines.

Owing to the VLA being in the “A” configuration, we obtained excellent image resolution of $0.42'' \times 0.21''$. However, *Swift* J195509.6+261406 was not detected and we get an upper limit of $7.3 \pm 31.5 \mu\text{Jy}$.

6. Archival Observations

A query of the *Simbad* database reveals no catalogued object within the BAT localization. The *INTEGRAL* observatory conducts regular scans of the Galactic plane and, in addition, performed several long pointed observations of the field around *Swift* J195509.6+261406. Over the past four years, this field has been observed with the IBIS instrument to total 1.5 Ms being within its fully-coded field-of-view (FCFOV, $9^\circ \times 9^\circ$) and up to 2.5 Ms being within the partially coded field-of-view ($29^\circ \times 29^\circ$). The efficiency of observations within the

FCFOV falls to zero at the field’s edge. The coverage of these 4 years by observations was non-uniform with the maximum exposure reached in the fall of 2006 (for FCFOV).

There is no reported source close to the transient’s position in the recent IBIS/ISGRI soft gamma-ray catalogs (Krivonos et al. 2007; Bird et al. 2007). We have also reanalyzed the archival data of *INTEGRAL* and failed to detect the source. A $4\text{-}\sigma$ limit of 0.9 mCrab in the 18–45 keV band (or 0.8 mCrab in the 17–60 keV band) has been received (flux of 1 mCrab corresponds to 1.1 and 1.4×10^{-11} erg cm $^{-2}$ s $^{-1}$ in these bands respectively for a source with Crab-like spectrum). There was also no source detected on a time scale of one individual pointing (2.0–3.6 ksec). We derive a $4\text{-}\sigma$ limit of ~ 20 mCrab.

Spitzer observed the position of *Swift* J195509.6+261406 during the Galactic Legacy Infrared Mid-Plane Survey Extraordinaire (GLIMPSE) on 2004 Oct 31st. Conservative upper limits for a source at the *K*-band position are 280, 350, 1700 and 6350 μ Jy at 3.6, 4.5, 5.8 and 8.0 μ m respectively.

7. Basic Considerations: Distance, Energetics and Radius

The fluence, the hardness and the duration of GRB 070610 are not atypical of GRBs. However, *Swift* J195509.6+261406 is an atypical afterglow in the X-ray band (§2). The optical counterpart is also atypical. Correcting for the total interstellar extinction along the line of sight, the apparent *i'*-band magnitude of the optical transient is as bright as ~ 13 mag more than a day after the burst trigger – there is no other optical extragalactic afterglow as bright at such late times.

The issue that faces us is quite simple: is GRB 070610 related to *Swift* J195509.6+261406? For extragalactic long-duration GRBs that the *Swift*-XRT was able to observe within an hour of the burst trigger, the overwhelming majority have a detected X-ray afterglow.

We therefore consider it unlikely that GRB 070610 arises from a background (i.e. extragalactic) event. The spatial and temporal coincidence of GRB 070610 and *Swift* J195509.6+261406 suggest that these are strongly related. If so, the event is of Galactic origin. Accepting this association we turn our attention to the fundamental parameters characterizing *Swift* J195509.6+261406.

The extinction estimate based on the full X-ray spectrum excluding the flare (see Table 1) corresponds to $E(B - V) = 1.0\text{--}1.5$ mag (Based on optical spectral classification of nearby stars, we find $E(B - V) \sim 1.1$). Assuming $R = 3.1$, this corresponds to $A_K = 0.4\text{--}0.5$ mag. The infrared *K'*-band magnitude of the NIR counterpart *Swift* J195509.6+261406 is

no brighter than ~ 21.5 (Table 3). From late-time optical observations, we also know that $R > 26.0$ (Table 2). Since the farthest distance for a star in the disk of our galaxy is 30 kpc, we get extinction-corrected absolute magnitude of $M_K > 3.6$ and $M_R > 4.8$. This clearly rules out the luminosity class of giants and supergiants (Cox 2000). This also constrains the spectral type to be cooler than G8 (Kraus & Hillenbrand 2007). If we assume a distance of 10 kpc, we can further constrain it to a spectral type cooler than M3. We also note here that in the case of another black-hole binary, XTE J1550-564, Orosz et al. (2002) find that the gravity is lower than the nominal gravity for dwarfs.

The prompt γ -ray burst peak flux is $5 \times 10^{-8} \text{ erg cm}^{-2}\text{s}^{-1}$, the peak X-ray flare flux is twice as faint and the mean flux over the first week is approximately a factor of 10^4 fainter than the burst peak flux. These translate to the following isotropic luminosities: $6 \times 10^{38} d_{10}^2 \text{ erg s}^{-1}$, $3 \times 10^{38} d_{10}^2 \text{ erg s}^{-1}$ and $5 \times 10^{34} d_{10}^2 \text{ erg s}^{-1}$.

The prompt gamma-rays can constrain the radius of the emission. The BAT burst duration of several seconds (see Figure 1) puts an upper limit on the size of the emitting region (along the line of sight) to be smaller than $\sim 10^{11} \beta_c \text{ cm}$, where β_c is the causal speed in units of the light speed (i.e, the speed in which information, such as sound, travels). Since we expect $\beta_c \ll 1$ in non-compact objects (e.g., main sequence stars) the source of the prompt gamma-rays is a black hole, a neutron star or a white dwarf (the sound crossing time of the latter is seconds).

On the other hand, the non-thermal gamma-rays can be used to put a lower limit on the emission radius. If the gamma-ray spectrum continues to high energy ($E > m_e c^2$) then pair production opacity starts playing a role. Using the formulation of Lithwick & Sari (2001) and assuming a non-relativistic source we find that the size of the emitting region has to be $\gtrsim L \sigma_T / (0.1 \pi m_e c^3) \approx 10^9 d_{10}^2 \text{ cm}$, where the approximated numerical factor (taken here as 0.1π) depends on the radiation spectrum and the geometry of the source (Svensson 1987). This radius implies that if the engine of the burst is a neutron star or a black hole then the observed gamma-rays are produced far from the engine by (possibly relativistic) ejecta.

8. A Curious Galactic Transient

With a compact object (§7) and a fainter than K-dwarf companion, *Swift* J195509.6+261406 is likely a binary system. We now turn our attention to investigate the mechanism powering the unusual emission, with an emphasis on identifying analogous systems in our Galaxy.

At first blush, soft γ -ray repeater (SGR) flares appear to be a viable model for *Swift* J195509.6+261406. SGR exhibits hard X-ray flares with durations ranging from 0.1 s to

10 s and isotropic luminosities of 10^{46} erg (Aptekar et al. 2001; Hurley et al. 2005). Furthermore, variable X-ray afterglows have been detected after several SGR outbursts (see e.g. Woods & Thompson 2006).

However, this interpretation has several problems. First, SGR flares lasting longer than 1 s, dubbed “intermediate” SGR flares, have an energy release $\approx 10^{41}$ erg, two orders of magnitude larger than our upper limit for *Swift* J195509.6+261406 (Woods & Thompson 2006). Second, pulsations are typically observed in SGR flare X-ray afterglows at the neutron star spin rate. We see no evidence for pulsations from *Swift* J195509.6+261406 (though constrained by the 2.5 s sampling interval). Finally, no known SGR has a companion. If *Swift* J195509.6+261406 were caused by an SGR flare, a cooler than K-dwarf companion would make *Swift* J195509.6+261406 the first binary magnetar.

Unlike SGR flares, the remaining possibilities are ultimately powered by accretion instead of magnetic activity (Arefiev et al. 2003 provide a comprehensive review of such transients in the hard X-ray sky). Cygnus X-1, a black hole binary with a supergiant companion, exhibits hard x-ray outbursts (Stern et al. 2001; Golenetskii et al. 2003). The *INTEGRAL* mission has identified a class of bright hard X-ray transients, the so-called Supergiant Fast X-ray Transients (SFXT; Negueruela et al. 2007). However, these events are relatively soft, and have timescales of 10^3 s or longer. Furthermore, the super-giant donor is an essential part of the SFXT story – the X-ray flares arise from accretion of “blobs” in the wind of the supergiant star. The faintness of the quiescent counterpart convincingly rules out the giant and supergiant scenarios.

The high peak luminosity strongly suggests an event like IC Cam (see Belloni et al. 1999). However, this too is a questionable analog for the reasons of the lack of a bright optical/NIR counterpart and also the short flare duration. For the same reasons, the analogy to A0538–66 (the well known Be-pulsar X-ray binary in the LMC) can also be ruled out.

The bursting pulsar GRO J1744–28 shares some properties with those from GRB 070610. From 1995–1997, thousands of bursts were detected by *BATSE* out to > 60 keV (Kouveliotou et al. 1996; Woods et al. 1999). The spectrum of the bursts in *BATSE* and *RXTE* was adequately modeled by a thermal bremsstrahlung model having $kT \sim 10$ keV; burst durations were approximately 10 s. GRO J1744–28 consists of a neutron star in an 11.8 d orbit with a low mass companion (Finger et al. 1996). However, unlike *Swift* J195509.6+261406, there is no evidence for a highly variable optical emission associated with these bursts. Also the high-energy bursts from GRO J1744–28 are highly repetitive. Searches for other episodes of emission from GRB 070610 did not yield any obvious candidates either in the BAT data or in the extensive *INTEGRAL* survey (§6) and the Interplanetary Network (§9).

The best analog to the X-ray and optical emission from *Swift* J195509.6+261406 is V4641 Sgr (Markwardt et al. 2007) – a transient which has been recognized by several authors as being one of the fastest transients in the hard X-ray (in’t Zand et al. 2000; Uemura et al. 2002; Arefiev et al. 2003). V4641 Sgr came to the attention of astronomers through a major outburst in 1999 (see in’t Zand et al. 2000). We now infer that this object is a binary consisting of a B9 III star orbiting a $9 M_{\odot}$ black hole (Orosz et al. 2001). The system exhibited strong and fast X-ray and optical variability – similar to what we see in *Swift* J195509.6+261406.

Rapid (< 100 s) and intense (modulation index, $S = \langle f \rangle / \Delta(f) \gtrsim 10$; here f is the X-ray flux and Δf is the variability in f) but with mean X-ray luminosity $\langle L \rangle$ that is well below Eddington flux mark V4641 Sgr from the other black hole binaries (Revnivtsev et al. 2002). The classical black hole LMXBs such as A0620–00 exhibit X-ray novae with peak super-Eddington flux and a decline over a month (see reviews by Tanaka & Shibazaki 1996; Remillard & McClintock 2006). Micro-quasars such as GRS 1915+10 exhibit intense variations (with S approaching ten) but only when $\langle L \rangle$ is extremely high, $\langle L \rangle \sim 10^{39}$ erg s $^{-1}$ (e.g. Belloni et al. 1997; Munro et al. 1999).

The first difference between *Swift* J195509.6+261406 and V4641 Sgr is the donor star: *Swift* J195509.6+261406 has a cool dwarf donor, while V4641 Sgr has a B9 giant donor. We suggest that the distinctive variability of V4641 Sgr arises from the black hole companion and has less to do with the nature of the donor star. This conjecture would allow us to infer that the compact object in *Swift* J195509.6+261406 is also a black hole. While V4641 Sgr seems to be the closest event we have to *Swift* J195509.6+261406, it is clear that no perfect analog to *Swift* J195509.6+261406 exists. In particular, there has been no report of a burst of gamma-rays from V4641 Sgr. However, the absence could be due to the short duration duty cycle of the gamma-ray bursts.

With two similar objects in hand—V4641 Sgr and GRB 070610—we now have the luxury of defining a new class of transients: fast X-ray novae which, in addition to the rapid X-ray and optical variability but at sub-Eddington luminosities, are also (apparently) marked by GRB-like bursts.

What differentiates fast X-ray novae from the regular X-ray novae? Regular X-ray novae are essentially black hole binaries undergoing the equivalent of dwarf novae i.e. instabilities in the disk. During the major burst of 1999, V4641 Sgr exhibited radio emission and relativistic motion (Hjellming et al. 2000). The radio flux of V4641 Sgr declined very steeply initially; from 360 mJy at 8.3 GHz to 30 mJy at 8.46 GHz in one day (Hjellming et al. 2000). According to Orosz et al. 2001, the distance to V4641 Sgr is 7.4–12.3 kpc and the apparent expansion velocity is $> 9.5c$ (assuming the lowest proper motion estimate from

Hjellming et al. 2000) – making V4641 Sgr the most relativistic of Galactic sources. This suggests that perhaps the key difference between fast X-ray novae and the regular X-ray novae is the speed at which the ejecta is emitted. Unfortunately, neither was GRB070610 as bright as V4641 Sgr in the optical and X-ray immediately after the flare nor were our radio observations undertaken promptly after the detection of GRB 070610 to verify this hypothesis.

9. Implications: Galactic GRBs

Spurred by the connection between *Swift* J195509.6+261406 with a Galactic transient we investigated whether this source or its analog V4641 Sgr emitted bursts of gamma-rays in the past. We have constructed a list of 1211 GRBs detected by the IPN (Hurley et al. 1999), whose position is constrained by at least one annulus with semi-width smaller than 0.5 deg. This catalog contains events observed from 1990 November 12, to 2005 October 31 (see Ofek 2007 for more details). We did not find any IPN GRB that coincides with either of these positions.

We also searched for *Swift*-BAT sub-threshold events which are consistent with the positions of V4641 Sgr and *Swift* J195509.6+261406. There is no BAT sub-threshold event within 5' from the location of V4641 Sgr. But, we find an event at a signal-to-noise ratio (SNR) of 5.0 located at RA=298.77°, Dec=+26.221° (1.8' from the position of GRB 070610) and occurring on UT 2006 Nov 17.7812. However, adjusted for the approximate number of times this field has been observed, the significance drops below 2- σ . We consider it likely this sub-threshold event is nothing more than a statistical fluctuation.

V4641 Sgr has been undergoing major bursts approximately every two years (see Uemura et al. 2004). The absence of a detection of a gamma-ray burst could simply be due to lack of coverage or that not all such bursting activity are preceded by a burst of gamma-rays.

Another possible member of this class of fast X-ray novae is XTEJ1901+014 (Karasev et al. 2007) which is potentially associated with GRB020406 (Remillard & Smith 2002).

Nonetheless, it is reasonable to speculate that a burst similar to *Swift* J195509.6+261406 occurs in our Galaxy, say, every decade. This alone immediately makes *Swift* J195509.6+261406 and related events as the most common of long-duration gamma-ray bursts. (The mean time between cosmological GRBs in our Galaxy is no smaller than 10^5 yr).

Several hundred years ago, optical astronomers put all new apparitions of stars as *novae stella*. Over the past century astronomers have shown that *novae stella* split into three

distinctly different phenomena: novae, supernovae of type Ia and core collapse supernovae. The novae, in turn, are divided into five families which arise from instabilities in the accretion disk feeding a white dwarf, neutron star or a black hole and on the surfaces of white dwarfs and neutron stars.

History is repeating itself. Only thirty years ago, astronomers referred to all bursts of gamma-ray radiation as GRBs. Over the last decade astronomers have established SHBs and LSBs to be of cosmological origin (Metzger et al. 1997; Gehrels et al. 2005; Bloom et al. 2006; Fox et al. 2005) and reasonably established their origin: coalescence of compact objects and deaths of massive stars respectively.

However, fissures are already developing. Recently, hypergiant flares from magnetars in our own Galaxy and nearby galaxies have been found to contaminate the SHB sample. The Galactic rate of the hypergiant flares is likely 10^{-3} yr^{-1} (Ofek 2007) much larger than the estimated Galactic SHB rate of 10^{-6} yr^{-1} (Nakar et al. 2006; Guetta & Piran 2006).

Our galaxy has at least two fast X-ray novae systems (V4641 Sgr and *Swift* J195509.6+261406). The rate of GRB 070610-like events (with no assumption about beaming) is likely to be about $3.5^{+8.0}_{-2.9} \text{ yr}^{-1}$ which is five orders of magnitude larger than the estimated cosmological GRBs rate. However, these events are yet unobservable outside our galaxy with the current limitation in sensitivity of high energy detectors. As usual the meekest events dominate the demography.

We thank M. van Kerkwijk for help with Keck observations and discussions. We thank J. Cohen, J. Simon, A. Kraus, M. Muno, E. S. Phinney and R. Narayan for valuable discussions. We also acknowledge D. Law, T. Treu and P. Marshall. As always we are grateful to the selfless librarians and astronomers who maintain the *Simbad* database. M. M. K. thanks the Gordon and Betty Moore Foundation for support with the George Ellory Hale Fellowship. S. B. C. and A. M. S. are supported by a NASA Graduate Student Research Fellowship. JSB is a Sloan Research Fellow and is partially supported by a Hellman Faculty Award. P. C. S. is supported by a Jansky Fellowship. E. B. is supported by a Hubble fellowship. GRB research at Caltech is supported in part by grants from NSF (AST program) and NASA (Swift and HST mission).

REFERENCES

- Aptekar, R. L., Frederiks, D. D., Golenetskii, S. V., Il’inskii, V. N., Mazets, E. P., Pal’shin, V. D., Butterworth, P. S., & Cline, T. L. 2001, *ApJS*, 137, 227
- Arefiev, V. A., Priedhorsky, W. C., & Borozdin, K. N. 2003, *ApJ*, 586, 1238
- Barthelmy, S. D., Barbier, L. M., Cummings, J. R., Fenimore, E. E., Gehrels, N., Hullinger, D., Krimm, H. A., Markwardt, C. B., Palmer, D. M., Parsons, A., Sato, G., Suzuki, M., Takahashi, T., Tashiro, M., & Tueller, J. 2005, *Space Science Reviews*, 120, 143
- Belloni, T., Dieters, S., van den Ancker, M. E., Fender, R. P., Fox, D. W., Harmon, B. A., van der Klis, M., Kommers, J. M., Lewin, W. H. G., & van Paradijs, J. 1999, *ApJ*, 527, 345
- Belloni, T., Mendez, M., King, A. R., van der Klis, M., & van Paradijs, J. 1997, *ApJ*, 488, L109+
- Bird, A. J., Malizia, A., Bazzano, A., Barlow, E. J., Bassani, L., Hill, A. B., Bélanger, G., Capitanio, F., Clark, D. J., Dean, A. J., Fiocchi, M., Götz, D., Lebrun, F., Molina, M., Produit, N., Renaud, M., Sguera, V., Stephen, J. B., Terrier, R., Ubertini, P., Walter, R., Winkler, C., & Zurita, J. 2007, *ApJS*, 170, 175
- Bloom, J. S., Prochaska, J. X., Pooley, D., Blake, C. H., Foley, R. J., Jha, S., Ramirez-Ruiz, E., Granot, J., Filippenko, A. V., Sigurdsson, S., Barth, A. J., Chen, H.-W., Cooper, M. C., Falco, E. E., Gal, R. R., Gerke, B. F., Gladders, M. D., Greene, J. E., Hennanwi, J., Ho, L. C., Hurley, K., Koester, B. P., Li, W., Lubin, L., Newman, J., Perley, D. A., Squires, G. K., & Wood-Vasey, W. M. 2006, *ApJ*, 638, 354
- Buccheri, R., Bennett, K., Bignami, G. F., Bloemen, J. B. G. M., Boriakoff, V., Caraveo, P. A., Hermsen, W., Kanbach, G., Manchester, R. N., Masnou, J. L., Mayer-Hasselwander, H. A., Ozel, M. E., Paul, J. A., Sacco, B., Scarsi, L., & Strong, A. W. 1983, *A&A*, 128, 245
- Burrows, D. N., Hill, J. E., Nousek, J. A., Kennea, J. A., Wells, A., Osborne, J. P., Abbey, A. F., Beardmore, A., Mukerjee, K., Short, A. D. T., Chincarini, G., Campana, S., Citterio, O., Moretti, A., Pagani, C., Tagliaferri, G., Giommi, P., Capalbi, M., Tamburelli, F., Angelini, L., Cusumano, G., Bräuninger, H. W., Burkert, W., & Hartner, G. D. 2005, *Space Science Reviews*, 120, 165
- Cardelli, J. A., Clayton, G. C., & Mathis, J. S. 1989, *ApJ*, 345, 245

- Cenko, S. B., Fox, D. B., Moon, D.-S., Harrison, F. A., Kulkarni, S. R., Henning, J. R., Guzman, C. D., Bonati, M., Smith, R. M., Thicksten, R. P., Doyle, M. W., Petrie, H. L., Gal-Yam, A., Soderberg, A. M., Anagnostou, N. L., & Laity, A. C. 2006, *PASP*, 118, 1396
- Chincarini, G., Moretti, A., Romano, P., Falcone, A. D., Morris, D., Racusin, J., Campana, S., Guidorzi, C., Tagliaferri, G., Burrows, D. N., Pagani, C., Stroh, M., Grupe, D., Capalbi, M., Cusumano, G., Gehrels, N., Giommi, P., La Parola, V., Mangano, V., Mineo, T., Nousek, J. A., O’Brien, P. T., Page, K. L., Perri, M., Troja, E., Willingale, R., & Zhang, B. 2007, *ArXiv Astrophysics e-prints*
- Cox, A. N. 2000, *Allen’s astrophysical quantities* (Allen’s astrophysical quantities, 4th ed. Publisher: New York: AIP Press; Springer, 2000. Edited by Arthur N. Cox. ISBN: 0387987460)
- Dickey, J. M. & Lockman, F. J. 1990, *ARA&A*, 28, 215
- Evans, P. A., Beardmore, A. P., Page, K. L., Tyler, L. G., Osborne, J. P., Goad, M. R., O’Brien, P. T., Vetere, L., Racusin, J., Morris, D., Burrows, D. N., Capalbi, M., Perri, M., Gehrels, N., & Romano, P. 2007, *A&A*, 469, 379
- Falcone, A. D., Burrows, D. N., Lazzati, D., Campana, S., Kobayashi, S., Zhang, B., Mészáros, P., Page, K. L., Kennea, J. A., Romano, P., Pagani, C., Angelini, L., Beardmore, A. P., Capalbi, M., Chincarini, G., Cusumano, G., Giommi, P., Goad, M. R., Godet, O., Grupe, D., Hill, J. E., La Parola, V., Mangano, V., Moretti, A., Nousek, J. A., O’Brien, P. T., Osborne, J. P., Perri, M., Tagliaferri, G., Wells, A. A., & Gehrels, N. 2006, *ApJ*, 641, 1010
- Finger, M. H., Koh, D. T., Nelson, R. W., Prince, T. A., Vaughan, B. A., & Wilson, R. B. 1996, *Nature*, 381, 291
- Fox, D. B., Frail, D. A., Price, P. A., Kulkarni, S. R., Berger, E., Piran, T., Soderberg, A. M., Cenko, S. B., Cameron, P. B., Gal-Yam, A., Kasliwal, M. M., Moon, D.-S., Harrison, F. A., Nakar, E., Schmidt, B. P., Penprase, B., Chevalier, R. A., Kumar, P., Roth, K., Watson, D., Lee, B. L., Sheckman, S., Phillips, M. M., Roth, M., McCarthy, P. J., Rauch, M., Cowie, L., Peterson, B. A., Rich, J., Kawai, N., Aoki, K., Kosugi, G., Totani, T., Park, H.-S., MacFadyen, A., & Hurley, K. C. 2005, *Nature*, 437, 845
- French, J., Melady, G., Kubanek, P., & Jelinek, M. 2007, *GCN Circular* 6500
- Gehrels, N., Chincarini, G., Giommi, P., Mason, K. O., Nousek, J. A., Wells, A. A., White, N. E., Barthelmy, S. D., Burrows, D. N., Cominsky, L. R., Hurley, K. C., Marshall,

- F. E., Mészáros, P., Roming, P. W. A., Angelini, L., Barbier, L. M., Belloni, T., Campana, S., Caraveo, P. A., Chester, M. M., Citterio, O., Cline, T. L., Cropper, M. S., Cummings, J. R., Dean, A. J., Feigelson, E. D., Fenimore, E. E., Frail, D. A., Fruchter, A. S., Garmire, G. P., Gendreau, K., Ghisellini, G., Greiner, J., Hill, J. E., Hunsberger, S. D., Krimm, H. A., Kulkarni, S. R., Kumar, P., Lebrun, F., Lloyd-Ronning, N. M., Markwardt, C. B., Mattson, B. J., Mushotzky, R. F., Norris, J. P., Osborne, J., Paczynski, B., Palmer, D. M., Park, H.-S., Parsons, A. M., Paul, J., Rees, M. J., Reynolds, C. S., Rhoads, J. E., Sasseen, T. P., Schaefer, B. E., Short, A. T., Smale, A. P., Smith, I. A., Stella, L., Tagliaferri, G., Takahashi, T., Tashiro, M., Townsley, L. K., Tueller, J., Turner, M. J. L., Vietri, M., Voges, W., Ward, M. J., Willingale, R., Zerbi, F. M., & Zhang, W. W. 2004, *ApJ*, 611, 1005
- Gehrels, N., Sarazin, C. L., O’Brien, P. T., Zhang, B., Barbier, L., Barthelmy, S. D., Blustin, A., Burrows, D. N., Cannizzo, J., Cummings, J. R., Goad, M., Holland, S. T., Hurkett, C. P., Kennea, J. A., Levan, A., Markwardt, C. B., Mason, K. O., Meszaros, P., Page, M., Palmer, D. M., Rol, E., Sakamoto, T., Willingale, R., Angelini, L., Beardmore, A., Boyd, P. T., Breeveld, A., Campana, S., Chester, M. M., Chincarini, G., Cominsky, L. R., Cusumano, G., de Pasquale, M., Fenimore, E. E., Giommi, P., Gronwall, C., Grupe, D., Hill, J. E., Hinshaw, D., Hjorth, J., Hullinger, D., Hurley, K. C., Klose, S., Kobayashi, S., Kouveliotou, C., Krimm, H. A., Mangano, V., Marshall, F. E., McGowan, K., Moretti, A., Mushotzky, R. F., Nakazawa, K., Norris, J. P., Nousek, J. A., Osborne, J. P., Page, K., Parsons, A. M., Patel, S., Perri, M., Poole, T., Romano, P., Roming, P. W. A., Rosen, S., Sato, G., Schady, P., Smale, A. P., Sollerman, J., Starling, R., Still, M., Suzuki, M., Tagliaferri, G., Takahashi, T., Tashiro, M., Tueller, J., Wells, A. A., White, N. E., & Wijers, R. A. M. J. 2005, *Nature*, 437, 851
- Golenetskii, S., Aptekar, R., Frederiks, D., Mazets, E., Palshin, V., Hurley, K., Cline, T., & Stern, B. 2003, *ApJ*, 596, 1113
- Guetta, D. & Piran, T. 2006, *A&A*, 453, 823
- Hjellming, R. M., Rupen, M. P., Hunstead, R. W., Campbell-Wilson, D., Mioduszewski, A. J., Gaensler, B. M., Smith, D. A., Sault, R. J., Fender, R. P., Spencer, R. E., de la Force, C. J., Richards, A. M. S., Garrington, S. T., Trushkin, S. A., Ghigo, F. D., Waltman, E. B., & McCollough, M. 2000, *ApJ*, 544, 977
- Hodapp, K. W., Jensen, J. B., Irwin, E. M., Yamada, H., Chung, R., Fletcher, K., Robertson, L., Hora, J. L., Simons, D. A., Mays, W., Nolan, R., Bec, M., Merrill, M., & Fowler, A. M. 2003, *PASP*, 115, 1388

- Hurley, K., Boggs, S. E., Smith, D. M., Duncan, R. C., Lin, R., Zoglauer, A., Krucker, S., Hurford, G., Hudson, H., Wigger, C., Hajdas, W., Thompson, C., Mitrofanov, I., Sanin, A., Boynton, W., Fellows, C., von Kienlin, A., Lichti, G., Rau, A., & Cline, T. 2005, *Nature*, 434, 1098
- Hurley, K., Briggs, M. S., Kippen, R. M., Kouveliotou, C., Meegan, C., Fishman, G., Cline, T., & Boer, M. 1999, *ApJS*, 120, 399
- in’t Zand, J. J. M., Kuulkers, E., Bazzano, A., Cornelisse, R., Cocchi, M., Heise, J., Muller, J. M., Natalucci, L., Smith, M. J. S., & Ubertini, P. 2000, *A&A*, 357, 520
- Kalberla, P. M. W., Burton, W. B., Hartmann, D., Arnal, E. M., Bajaja, E., Morras, R., & Pöppel, W. G. L. 2005, *A&A*, 440, 775
- Kann, D. A., Wilson, A. C., Schulze, S., Klose, S., Henze, M., Ludwig, F., Laux, U., & Greiner, J. 2007, *GCN Circular* 6505
- Karasev, D. I., Lutovinov, A. A., & Grebenev, S. A. 2007, *Astronomy Letters*, 33, 159
- Klotz, K. A., Boer, B. M., Atteia, A. J. L., & Gendre, G. B. 2007, *GCN Circular* 6513
- Kouveliotou, C., van Paradijs, J., Fishman, G. J., Briggs, M. S., Kommers, J., Harmon, B. A., Meegan, C. A., & Lewin, W. H. G. 1996, *Nature*, 379, 799
- Kraus, A. L. & Hillenbrand, L. A. 2007, *ArXiv e-prints*, 708
- Krivonos, R., Revnivtsev, M., Lutovinov, A., Sazonov, S., Churazov, E., & Sunyaev, R. 2007, *ArXiv Astrophysics e-prints*
- Lithwick, Y. & Sari, R. 2001, *ApJ*, 555, 540
- Markwardt, C. B., Pagani, C., Evans, P., Gavriil, F. P., Kennea, J. A., Krimm, H. A., Landsman, W., & Marshall, F. E. 2007, *The Astronomer’s Telegram*, 1102, 1
- Metzger, M. R., Djorgovski, S. G., Kulkarni, S. R., Steidel, C. C., Adelberger, K. L., Frail, D. A., Costa, E., & Frontera, F. 1997, *Nature*, 387, 878
- Munari, U., Sordo, R., Castelli, F., & Zwitter, T. 2005, *A&A*, 442, 1127
- Muno, M. P., Morgan, E. H., & Remillard, R. A. 1999, *ApJ*, 527, 321
- Nakar, E., Gal-Yam, A., & Fox, D. B. 2006, *ApJ*, 650, 281
- Negueruela, I., Smith, D. M., Torrejon, J. M., & Reig, P. 2007, *ArXiv e-prints*, 704

- Norris, J. P., Nemiroff, R. J., Bonnell, J. T., Scargle, J. D., Kouveliotou, C., Paciesas, W. S., Meegan, C. A., & Fishman, G. J. 1996, *ApJ*, 459, 393
- Nousek, J. A., Kouveliotou, C., Grupe, D., Page, K. L., Granot, J., Ramirez-Ruiz, E., Patel, S. K., Burrows, D. N., Mangano, V., Barthelmy, S., Beardmore, A. P., Campana, S., Capalbi, M., Chincarini, G., Cusumano, G., Falcone, A. D., Gehrels, N., Giommi, P., Goad, M. R., Godet, O., Hurkett, C. P., Kennea, J. A., Moretti, A., O’Brien, P. T., Osborne, J. P., Romano, P., Tagliaferri, G., & Wells, A. A. 2006, *ApJ*, 642, 389
- Ofek, E. O. 2007, *ApJ*, 659, 339
- Oke, J. B., Cohen, J. G., Carr, M., Cromer, J., Dingizian, A., Harris, F. H., Labrecque, S., Lucinio, R., Schaal, W., Epps, H., & Miller, J. 1995, *PASP*, 107, 375
- Orosz, J. A., Groot, P. J., van der Klis, M., McClintock, J. E., Garcia, M. R., Zhao, P., Jain, R. K., Bailyn, C. D., & Remillard, R. A. 2002, *ApJ*, 568, 845
- Orosz, J. A., Kuulkers, E., van der Klis, M., McClintock, J. E., Garcia, M. R., Callanan, P. J., Bailyn, C. D., Jain, R. K., & Remillard, R. A. 2001, *ApJ*, 555, 489
- Pagani, C., Barthelmy, S. D., Cummings, J. R., Gehrels, N., Grupe, D., Holland, S. T., Kennea, J. A., Markwardt, C. B., Marshall, F. E., O’Brien, P. T., Palmer, D. M., Parsons, A. M., Stamatikos, M., & Vetere, L. 2007a, *GCN Circular* 6489
- Pagani, C., Racusin, J. L., & Kennea, J. A. 2007b, *GCN Circular* 6506
- Postigo, A. d. U., Castro-Tirado, A. J., & Aceituno, F. 2007, *GCN Circular* 6501
- Remillard, R. A. & McClintock, J. E. 2006, *ARA&A*, 44, 49
- Remillard, R. A. & Smith, D. 2002, *Atel* 88
- Revnivtsev, M., Gilfanov, M., Churazov, E., & Sunyaev, R. 2002, *A&A*, 391, 1013
- Schlegel, D. J., Finkbeiner, D. P., & Davis, M. 1998, *ApJ*, 500, 525
- Skrutskie, M. F., Cutri, R. M., Stiening, R., Weinberg, M. D., Schneider, S., Carpenter, J. M., Beichman, C., Capps, R., Chester, T., Elias, J., Huchra, J., Liebert, J., Lonsdale, C., Monet, D. G., Price, S., Seitzer, P., Jarrett, T., Kirkpatrick, J. D., Gizis, J. E., Howard, E., Evans, T., Fowler, J., Fullmer, L., Hurt, R., Light, R., Kopan, E. L., Marsh, K. A., McCallon, H. L., Tam, R., Van Dyk, S., & Wheelock, S. 2006, *AJ*, 131, 1163

- Stefanescu, A., Slowikowska, A., Kanbach, G., Duscha, S., Schrey, F., Steinle, H., & Ioannou, Z. 2007a, GCN Circular 6492
- Stefanescu, A., Slowikowska, A., Kanbach, G., et al. 2007b, GCN Circular 6508
- . 2007c, GCN Circular 6532
- Stern, B. E., Beloborodov, A. M., & Poutanen, J. 2001, *ApJ*, 555, 829
- Svensson, R. 1987, *MNRAS*, 227, 403
- Tanaka, Y. & Shibazaki, N. 1996, *ARA&A*, 34, 607
- Tueller, J., Barbier, L., Barthelmy, S. D., Cummings, J., Fenimore, E., Gehrels, N., Krimm, H., Markwardt, C., Pagani, C., Palmer, D., Parsons, A., Sakamoto, T., Sato, G., Stamatikos, M., & Ukwatta, T. 2007, GCN Circular 6491
- Uemura, M., Kato, T., Ishioka, R., Imada, A., Nogami, D., Monard, B., Cook, L. M., Stubbings, R., Kiyota, S., Nelson, P., Beninger, J.-Y., Bolt, G., & Heathcote, B. 2004, *PASJ*, 56, 823
- Uemura, M., Kato, T., Watanabe, T., Stubbings, R., Monard, B., & Kawai, N. 2002, *PASJ*, 54, 95
- Utdike, A. C., Hartmann, D. H., Henson, G., et al. 2007a, GCN Circular 6507
- Utdike, A. C., Milne, P. A., Williams, G. G., et al. 2007b, GCN Circular 6536
- van Dam, M. A., Bouchez, A. H., Le Mignant, D., Johansson, E. M., Wizinowich, P. L., Campbell, R. D., Chin, J. C. Y., Hartman, S. K., Lafon, R. E., Stomski, Jr., P. J., & Summers, D. M. 2006, *PASP*, 118, 310
- Wilson, J. C., Eikenberry, S. S., Henderson, C. P., Hayward, T. L., Carson, J. C., Pirger, B., Barry, D. J., Brandl, B. R., Houck, J. R., Fitzgerald, G. J., & Stolberg, T. M. 2003, in Presented at the Society of Photo-Optical Instrumentation Engineers (SPIE) Conference, Vol. 4841, Instrument Design and Performance for Optical/Infrared Ground-based Telescopes. Edited by Iye, Masanori; Moorwood, Alan F. M. Proceedings of the SPIE, Volume 4841, pp. 451-458 (2003)., ed. M. Iye & A. F. M. Moorwood, 451–458
- Wizinowich, P. L., Chin, J., Johansson, E., Kellner, S., Lafon, R., Le Mignant, D., Neyman, C., Stomski, P., Summers, D., Sumner, R., & van Dam, M. 2006, in Presented at the Society of Photo-Optical Instrumentation Engineers (SPIE) Conference, Vol. 6272, Advances in Adaptive Optics II. Edited by Ellerbroek, Brent L.; Bonaccini Calia, Domenico. Proceedings of the SPIE, Volume 6272, pp. 627209 (2006).

- Woods, P. M., Kouveliotou, C., van Paradijs, J., Briggs, M. S., Wilson, C. A., Deal, K., Harmon, B. A., Fishman, G. J., Lewin, W. H. G., & Kommers, J. 1999, *ApJ*, 517, 431
- Woods, P. M. & Thompson, C. 2006, Soft gamma repeaters and anomalous X-ray pulsars: magnetar candidates (Compact stellar X-ray sources), 547–586
- Yoshida, M., Yanagisawa, K., Shimizu, Y., et al. 2007, *GCN Circular* 6512
- Zhang, B., Fan, Y. Z., Dyks, J., Kobayashi, S., Mészáros, P., Burrows, D. N., Nousek, J. A., & Gehrels, N. 2006, *ApJ*, 642, 354

Table 5. Optical Observations of *Swift* J195509.6+261406 with Palomar 60-inch telescope

Epoch (2007 UT)	Facility	Filter	Time Since Burst (hr)	Exposure (s)	Magnitude
June 12.2416	P60	i'	32.92	30.0×1	19.1 ± 0.14
June 12.2422	P60	i'	32.94	30.0×1	>19.8
June 12.2433	P60	i'	32.96	30.0×3	>19.8
June 12.2444	P60	i'	32.99	30.0×5	19.7 ± 0.16
June 12.2450	P60	i'	33.00	30.0×5	19.6 ± 0.15
June 12.2456	P60	i'	33.02	30.0×5	19.6 ± 0.15
June 12.2462	P60	i'	33.03	30.0×5	19.7 ± 0.15
June 12.2467	P60	i'	33.05	30.0×5	>19.8
June 12.2473	P60	i'	33.06	30.0×5	>19.8
June 12.2479	P60	i'	33.07	30.0×5	>19.8
June 12.2484	P60	i'	33.09	30.0×1	>19.8
June 12.2484	P60	i'	33.09	30.0×5	>19.8
June 12.2490	P60	i'	33.10	30.0×1	18.9 ± 0.13
June 12.2496	P60	i'	33.11	30.0×1	18.7 ± 0.12
June 12.2501	P60	i'	33.13	30.0×1	>19.8
June 12.2513	P60	i'	33.15	30.0×5	>19.8
June 12.2518	P60	i'	33.17	30.0×3	19.8 ± 0.18
June 12.2518	P60	i'	33.17	30.0×5	19.7 ± 0.17
June 12.2524	P60	i'	33.18	30.0×3	19.7 ± 0.16
June 12.2529	P60	i'	33.19	30.0×3	19.7 ± 0.16
June 12.2541	P60	i'	33.22	30.0×5	>19.9
June 12.2547	P60	i'	33.23	30.0×1	>19.8
June 12.2547	P60	i'	33.23	30.0×5	>19.9
June 12.2552	P60	i'	33.25	30.0×1	18.5 ± 0.14
June 12.2558	P60	i'	33.26	30.0×1	>19.8
June 12.2569	P60	i'	33.29	30.0×1	>19.9
June 12.2569	P60	i'	33.29	30.0×3	>19.9
June 12.2569	P60	i'	33.29	30.0×5	>19.9
June 12.2575	P60	i'	33.30	30.0×1	19.2 ± 0.15
June 12.2581	P60	i'	33.32	30.0×1	19.8 ± 0.17
June 12.2598	P60	i'	33.36	30.0×5	19.9 ± 0.16
June 12.2604	P60	i'	33.37	30.0×5	>19.9
June 12.2610	P60	i'	33.39	30.0×5	>19.9
June 12.2615	P60	i'	33.40	30.0×5	>19.9
June 12.2621	P60	i'	33.41	30.0×5	>20.0

Table 5—Continued

Epoch (2007 UT)	Facility	Filter	Time Since Burst (hr)	Exposure (s)	Magnitude
June 12.2626	P60	i'	33.43	30.0×5	>20.0
June 12.2632	P60	i'	33.44	30.0×3	19.9 ± 0.16
June 12.2632	P60	i'	33.44	30.0×5	>20.0
June 12.2638	P60	i'	33.45	30.0×3	19.7 ± 0.16
June 12.2644	P60	i'	33.47	30.0×3	19.6 ± 0.15
June 12.2649	P60	i'	33.48	30.0×3	19.8 ± 0.16
June 12.2655	P60	i'	33.50	30.0×3	19.9 ± 0.17
June 12.2666	P60	i'	33.52	30.0×3	>20.0
June 12.2666	P60	i'	33.52	30.0×5	19.8 ± 0.16
June 12.2678	P60	i'	33.55	30.0×1	19.4 ± 0.14
June 12.2678	P60	i'	33.55	30.0×3	>20.0
June 12.2678	P60	i'	33.55	30.0×5	19.9 ± 0.16
June 12.2689	P60	i'	33.58	30.0×3	19.9 ± 0.17
June 12.3132	P60	i'	34.64	30.0×3	20.2 ± 0.19
June 12.3225	P60	i'	34.86	30.0×3	>20.4
June 12.3230	P60	i'	34.88	30.0×3	19.9 ± 0.16
June 12.3236	P60	i'	34.89	30.0×3	20.1 ± 0.16
June 12.3242	P60	i'	34.90	30.0×3	20.3 ± 0.19
June 12.3247	P60	i'	34.92	30.0×3	20.3 ± 0.19
June 12.3253	P60	i'	34.93	30.0×1	>20.3
June 12.3253	P60	i'	34.93	30.0×3	20.2 ± 0.19
June 12.3259	P60	i'	34.94	30.0×1	19.1 ± 0.13
June 12.3265	P60	i'	34.96	30.0×1	19.4 ± 0.14
June 12.3270	P60	i'	34.97	30.0×1	>20.3
June 12.3288	P60	i'	35.01	30.0×5	>20.3
June 12.3293	P60	i'	35.03	30.0×5	>20.3
June 12.3299	P60	i'	35.04	30.0×5	>20.3
June 12.3305	P60	i'	35.05	30.0×5	>20.4
June 12.3311	P60	i'	35.07	30.0×5	20.3 ± 0.17
June 12.3316	P60	i'	35.08	30.0×5	20.2 ± 0.18
June 12.3322	P60	i'	35.10	30.0×5	>20.4
June 12.3328	P60	i'	35.11	30.0×5	>20.5
June 12.3334	P60	i'	35.12	30.0×5	>20.5
June 12.3339	P60	i'	35.14	30.0×3	20.4 ± 0.17
June 12.3339	P60	i'	35.14	30.0×5	20.2 ± 0.17
June 12.3345	P60	i'	35.15	30.0×3	20.3 ± 0.18

Table 5—Continued

Epoch (2007 UT)	Facility	Filter	Time Since Burst (hr)	Exposure (s)	Magnitude
June 12.3351	P60	i'	35.17	30.0×3	20.1 ± 0.16
June 12.3357	P60	i'	35.18	30.0×3	20.3 ± 0.17
June 12.3363	P60	i'	35.19	30.0×1	20.2 ± 0.20
June 12.3363	P60	i'	35.19	30.0×3	20.1 ± 0.17
June 12.3369	P60	i'	35.21	30.0×1	19.7 ± 0.17
June 12.3380	P60	i'	35.24	30.0×3	20.0 ± 0.17
June 12.3386	P60	i'	35.25	30.0×3	20.3 ± 0.17
June 12.3392	P60	i'	35.26	30.0×1	>20.3
June 12.3392	P60	i'	35.26	30.0×3	20.3 ± 0.19
June 12.3397	P60	i'	35.28	30.0×1	19.1 ± 0.13
June 12.3403	P60	i'	35.29	30.0×1	>20.3
June 12.3409	P60	i'	35.30	30.0×1	>20.3
June 12.3420	P60	i'	35.33	30.0×1	20.0 ± 0.16
June 12.3420	P60	i'	35.33	30.0×3	20.0 ± 0.15
June 12.3432	P60	i'	35.36	30.0×3	20.1 ± 0.17
June 12.3443	P60	i'	35.39	30.0×5	>20.4
June 12.3449	P60	i'	35.40	30.0×5	>20.4
June 12.3455	P60	i'	35.42	30.0×3	20.2 ± 0.18
June 12.3455	P60	i'	35.42	30.0×5	20.2 ± 0.18
June 12.3466	P60	i'	35.44	30.0×5	20.2 ± 0.18
June 12.3472	P60	i'	35.46	30.0×5	>20.3
June 12.3478	P60	i'	35.47	30.0×5	>20.3
June 12.3484	P60	i'	35.48	30.0×5	>20.3
June 12.3490	P60	i'	35.50	30.0×5	>20.3
June 12.3495	P60	i'	35.51	30.0×1	>20.3
June 12.3495	P60	i'	35.51	30.0×5	>20.4
June 12.3501	P60	i'	35.53	30.0×1	>20.3
June 12.3507	P60	i'	35.54	30.0×1	>20.3
June 12.3513	P60	i'	35.55	30.0×1	>20.2
June 12.3524	P60	i'	35.58	30.0×5	>20.4
June 12.3530	P60	i'	35.60	30.0×5	>20.3
June 12.3536	P60	i'	35.61	30.0×5	>20.4
June 12.3542	P60	i'	35.62	30.0×5	>20.4
June 12.3547	P60	i'	35.64	30.0×5	>20.4
June 12.3553	P60	i'	35.65	30.0×5	>20.4
June 12.3559	P60	i'	35.66	30.0×5	20.4 ± 0.18

Table 5—Continued

Epoch (2007 UT)	Facility	Filter	Time Since Burst (hr)	Exposure (s)	Magnitude
June 12.3565	P60	i'	35.68	30.0×5	20.3 ± 0.18
June 12.3571	P60	i'	35.69	30.0×5	20.3 ± 0.18
June 12.3576	P60	i'	35.71	30.0×5	>20.3
June 12.3582	P60	i'	35.72	30.0×5	>20.3
June 12.3588	P60	i'	35.73	30.0×3	20.3 ± 0.17
June 12.3588	P60	i'	35.73	30.0×5	20.3 ± 0.17
June 12.3594	P60	i'	35.75	30.0×3	20.2 ± 0.18
June 12.3605	P60	i'	35.78	30.0×5	20.2 ± 0.18
June 12.3611	P60	i'	35.79	30.0×5	20.3 ± 0.18
June 12.3617	P60	i'	35.80	30.0×5	>20.4
June 12.3623	P60	i'	35.82	30.0×5	20.3 ± 0.18
June 12.3628	P60	i'	35.83	30.0×3	20.3 ± 0.20
June 12.3628	P60	i'	35.83	30.0×5	20.1 ± 0.18
June 12.3635	P60	i'	35.85	30.0×3	20.1 ± 0.18
June 12.3641	P60	i'	35.86	30.0×3	20.0 ± 0.17
June 12.3646	P60	i'	35.87	30.0×3	20.2 ± 0.18
June 12.3652	P60	i'	35.89	30.0×3	>20.4
June 12.3658	P60	i'	35.90	30.0×3	20.2 ± 0.17
June 12.3670	P60	i'	35.93	30.0×1	>20.4
June 12.3670	P60	i'	35.93	30.0×3	19.9 ± 0.16
June 12.3676	P60	i'	35.95	30.0×1	20.0 ± 0.16
June 12.3682	P60	i'	35.96	30.0×1	20.2 ± 0.19
June 12.3694	P60	i'	35.99	30.0×3	20.3 ± 0.18
June 12.3700	P60	i'	36.00	30.0×3	20.2 ± 0.16
June 12.3705	P60	i'	36.02	30.0×3	20.0 ± 0.16
June 12.3711	P60	i'	36.03	30.0×3	20.0 ± 0.16
June 12.3717	P60	i'	36.04	30.0×1	>20.4
June 12.3717	P60	i'	36.04	30.0×3	>20.4
June 12.3729	P60	i'	36.07	30.0×3	20.2 ± 0.19
June 12.3735	P60	i'	36.09	30.0×3	20.2 ± 0.17
June 12.3740	P60	i'	36.10	30.0×3	>20.4
June 12.3746	P60	i'	36.11	30.0×3	20.3 ± 0.17
June 12.3752	P60	i'	36.13	30.0×1	>20.4
June 12.3752	P60	i'	36.13	30.0×3	20.2 ± 0.18
June 12.3764	P60	i'	36.16	30.0×3	20.3 ± 0.18
June 12.3776	P60	i'	36.18	30.0×5	20.3 ± 0.17

Table 5—Continued

Epoch (2007 UT)	Facility	Filter	Time Since Burst (hr)	Exposure (s)	Magnitude
June 12.3782	P60	i'	36.20	30.0×1	>20.4
June 12.3782	P60	i'	36.20	30.0×5	>20.4
June 12.3787	P60	i'	36.21	30.0×1	16.7 ± 0.12
June 12.3793	P60	i'	36.23	30.0×1	19.2 ± 0.12
June 12.3799	P60	i'	36.24	30.0×1	19.0 ± 0.13
June 12.3805	P60	i'	36.26	30.0×1	>20.4
June 12.3817	P60	i'	36.28	30.0×3	20.0 ± 0.16
June 12.3817	P60	i'	36.28	30.0×5	20.4 ± 0.17
June 12.3823	P60	i'	36.30	30.0×3	20.3 ± 0.18
June 12.3829	P60	i'	36.31	30.0×3	20.3 ± 0.18
June 12.3840	P60	i'	36.34	30.0×1	>20.4
June 12.3840	P60	i'	36.34	30.0×3	>20.4
June 12.3840	P60	i'	36.34	30.0×5	20.3 ± 0.18
June 12.3846	P60	i'	36.35	30.0×1	18.5 ± 0.13
June 12.3852	P60	i'	36.37	30.0×1	19.9 ± 0.16
June 12.3858	P60	i'	36.38	30.0×1	>20.5
June 12.3869	P60	i'	36.41	30.0×3	20.0 ± 0.17
June 12.3875	P60	i'	36.42	30.0×3	20.1 ± 0.17
June 12.3881	P60	i'	36.44	30.0×1	>20.5
June 12.3881	P60	i'	36.44	30.0×3	20.2 ± 0.19
June 12.3887	P60	i'	36.45	30.0×1	17.5 ± 0.11
June 12.3893	P60	i'	36.47	30.0×1	19.3 ± 0.14
June 12.3899	P60	i'	36.48	30.0×1	>20.4
June 12.3917	P60	i'	36.52	30.0×5	20.3 ± 0.17
June 12.3923	P60	i'	36.54	30.0×3	20.3 ± 0.18
June 12.3923	P60	i'	36.54	30.0×5	20.3 ± 0.17
June 12.3935	P60	i'	36.57	30.0×5	20.4 ± 0.18
June 12.3940	P60	i'	36.58	30.0×5	20.4 ± 0.19
June 12.3946	P60	i'	36.59	30.0×1	>20.4
June 12.3946	P60	i'	36.59	30.0×5	20.4 ± 0.19
June 12.3952	P60	i'	36.61	30.0×1	19.6 ± 0.15
June 12.3958	P60	i'	36.62	30.0×1	20.0 ± 0.15
June 12.3970	P60	i'	36.65	30.0×3	20.3 ± 0.19
June 12.3970	P60	i'	36.65	30.0×5	20.4 ± 0.19
June 12.3976	P60	i'	36.67	30.0×3	20.3 ± 0.19
June 12.3982	P60	i'	36.68	30.0×1	>20.4

Table 5—Continued

Epoch (2007 UT)	Facility	Filter	Time Since Burst (hr)	Exposure (s)	Magnitude
June 12.3982	P60	i'	36.68	30.0×3	20.4 ± 0.18
June 12.3988	P60	i'	36.69	30.0×1	18.7 ± 0.13
June 12.3993	P60	i'	36.71	30.0×1	>20.5
June 12.4005	P60	i'	36.74	30.0×3	20.2 ± 0.18
June 12.4011	P60	i'	36.75	30.0×3	20.3 ± 0.19
June 12.4017	P60	i'	36.76	30.0×3	20.4 ± 0.18
June 12.4029	P60	i'	36.79	30.0×5	20.5 ± 0.19
June 12.4035	P60	i'	36.81	30.0×5	20.4 ± 0.19
June 12.4041	P60	i'	36.82	30.0×3	20.3 ± 0.18
June 12.4041	P60	i'	36.82	30.0×5	20.3 ± 0.18
June 12.4047	P60	i'	36.84	30.0×3	20.1 ± 0.18
June 12.4052	P60	i'	36.85	30.0×1	>20.5
June 12.4052	P60	i'	36.85	30.0×3	>20.5
June 12.4058	P60	i'	36.86	30.0×1	>20.6
June 12.4064	P60	i'	36.88	30.0×1	>20.6
June 12.4070	P60	i'	36.89	30.0×1	>20.6
June 12.4076	P60	i'	36.91	30.0×1	>20.6
June 12.4082	P60	i'	36.92	30.0×1	>20.6
June 12.4088	P60	i'	36.93	30.0×1	>20.7
June 12.4094	P60	i'	36.95	30.0×1	>20.7
June 12.4118	P60	i'	37.01	30.0×5	20.5 ± 0.18
June 12.4124	P60	i'	37.02	30.0×5	20.5 ± 0.18
June 12.4130	P60	i'	37.03	30.0×5	20.7 ± 0.20
June 12.4136	P60	i'	37.05	30.0×3	20.5 ± 0.17
June 12.4136	P60	i'	37.05	30.0×5	20.7 ± 0.20
June 12.4142	P60	i'	37.06	30.0×3	20.6 ± 0.19
June 12.4153	P60	i'	37.09	30.0×5	20.5 ± 0.19
June 12.4159	P60	i'	37.11	30.0×5	>20.7
June 12.4165	P60	i'	37.12	30.0×3	20.6 ± 0.20
June 12.4165	P60	i'	37.12	30.0×5	20.7 ± 0.21
June 12.4171	P60	i'	37.13	30.0×1	>20.7
June 12.4171	P60	i'	37.13	30.0×3	20.5 ± 0.18
June 12.4177	P60	i'	37.15	30.0×1	>20.7
June 12.4183	P60	i'	37.16	30.0×1	>20.7
June 12.4195	P60	i'	37.19	30.0×1	>20.6
June 12.4195	P60	i'	37.19	30.0×3	20.6 ± 0.19

Table 5—Continued

Epoch (2007 UT)	Facility	Filter	Time Since Burst (hr)	Exposure (s)	Magnitude
June 12.4201	P60	i'	37.21	30.0×1	19.6 ± 0.15
June 12.4207	P60	i'	37.22	30.0×1	20.4 ± 0.20
June 12.4219	P60	i'	37.25	30.0×1	20.0 ± 0.19
June 12.4219	P60	i'	37.25	30.0×3	20.0 ± 0.17
June 12.4225	P60	i'	37.26	30.0×1	19.3 ± 0.14
June 12.4231	P60	i'	37.28	30.0×1	20.4 ± 0.18
June 12.4243	P60	i'	37.31	30.0×3	20.5 ± 0.18
June 12.4249	P60	i'	37.32	30.0×3	>20.7
June 12.4255	P60	i'	37.33	30.0×1	>20.6
June 12.4255	P60	i'	37.33	30.0×3	20.6 ± 0.21
June 12.4261	P60	i'	37.35	30.0×1	>20.6
June 12.4267	P60	i'	37.36	30.0×1	>20.6
June 12.4273	P60	i'	37.38	30.0×1	>20.6
June 12.4279	P60	i'	37.39	30.0×1	19.6 ± 0.15
June 12.4285	P60	i'	37.41	30.0×1	>20.6
June 12.4291	P60	i'	37.42	30.0×1	>20.6
June 12.4297	P60	i'	37.44	30.0×1	19.7 ± 0.14
June 12.4303	P60	i'	37.45	30.0×1	19.8 ± 0.16
June 12.4309	P60	i'	37.46	30.0×1	>20.6
June 12.4321	P60	i'	37.49	30.0×3	20.4 ± 0.19
June 12.4327	P60	i'	37.51	30.0×1	>20.5
June 12.4327	P60	i'	37.51	30.0×3	>20.6
June 12.4333	P60	i'	37.52	30.0×1	19.6 ± 0.13
June 12.4339	P60	i'	37.54	30.0×1	19.8 ± 0.14
June 12.4345	P60	i'	37.55	30.0×1	>20.5
June 12.4357	P60	i'	37.58	30.0×3	20.4 ± 0.19
June 12.4363	P60	i'	37.59	30.0×3	20.6 ± 0.20
June 12.4368	P60	i'	37.61	30.0×1	>20.6
June 12.4368	P60	i'	37.61	30.0×3	20.5 ± 0.19
June 12.4374	P60	i'	37.62	30.0×1	18.5 ± 0.13
June 12.4540	P60	i'	38.02	30.0×1	20.1 ± 0.18
June 12.4552	P60	i'	38.05	30.0×3	20.4 ± 0.18
June 12.4557	P60	i'	38.06	30.0×3	20.4 ± 0.18
June 12.4563	P60	i'	38.08	30.0×1	20.2 ± 0.19
June 12.4563	P60	i'	38.08	30.0×3	20.2 ± 0.17
June 12.4570	P60	i'	38.09	30.0×1	19.9 ± 0.18

Table 5—Continued

Epoch (2007 UT)	Facility	Filter	Time Since Burst (hr)	Exposure (s)	Magnitude
June 12.4576	P60	i'	38.10	30.0×1	20.4 ± 0.18
June 12.4582	P60	i'	38.12	30.0×1	20.1 ± 0.20
June 12.4588	P60	i'	38.13	30.0×1	>20.4
June 12.4594	P60	i'	38.15	30.0×1	19.9 ± 0.17
June 12.4600	P60	i'	38.16	30.0×1	19.6 ± 0.15
June 12.4606	P60	i'	38.18	30.0×1	>20.4
June 12.4618	P60	i'	38.21	30.0×3	20.0 ± 0.17
June 12.4624	P60	i'	38.22	30.0×3	20.2 ± 0.17
June 12.4630	P60	i'	38.24	30.0×3	20.4 ± 0.18
June 12.4636	P60	i'	38.25	30.0×3	20.2 ± 0.16
June 12.4642	P60	i'	38.26	30.0×1	>20.4
June 12.4642	P60	i'	38.26	30.0×3	20.0 ± 0.15
June 12.4648	P60	i'	38.28	30.0×1	20.4 ± 0.20
June 12.4654	P60	i'	38.29	30.0×1	19.0 ± 0.13
June 12.4660	P60	i'	38.31	30.0×1	20.1 ± 0.16
June 12.4666	P60	i'	38.32	30.0×1	20.3 ± 0.18
June 12.4679	P60	i'	38.35	30.0×3	20.1 ± 0.17
June 12.4685	P60	i'	38.37	30.0×3	20.2 ± 0.18
June 12.4691	P60	i'	38.38	30.0×1	>20.4
June 12.4691	P60	i'	38.38	30.0×3	20.1 ± 0.17
June 12.4703	P60	i'	38.41	30.0×3	20.0 ± 0.16
June 12.4709	P60	i'	38.43	30.0×3	20.0 ± 0.17
June 12.4715	P60	i'	38.44	30.0×3	>20.4
June 12.4721	P60	i'	38.45	30.0×3	20.2 ± 0.18
June 12.4727	P60	i'	38.47	30.0×3	20.0 ± 0.15
June 12.4733	P60	i'	38.48	30.0×3	20.0 ± 0.15
June 12.4739	P60	i'	38.50	30.0×3	20.1 ± 0.16
June 12.4748	P60	i'	38.52	30.0×3	20.2 ± 0.17
June 12.4754	P60	i'	38.53	30.0×3	20.2 ± 0.18
June 12.4766	P60	i'	38.56	30.0×5	20.1 ± 0.18
June 12.4772	P60	i'	38.58	30.0×5	20.2 ± 0.18
June 12.4778	P60	i'	38.59	30.0×3	20.1 ± 0.17
June 12.4778	P60	i'	38.59	30.0×5	20.2 ± 0.17
June 12.4784	P60	i'	38.61	30.0×3	20.1 ± 0.17
June 12.4790	P60	i'	38.62	30.0×3	19.7 ± 0.15
June 12.4796	P60	i'	38.63	30.0×1	>20.0

Table 5—Continued

Epoch (2007 UT)	Facility	Filter	Time Since Burst (hr)	Exposure (s)	Magnitude
June 12.4796	P60	i'	38.63	30.0×3	>20.1
June 12.4816	P60	i'	38.68	30.0×5	>19.8
June 12.4822	P60	i'	38.70	30.0×1	19.4 ± 0.15
June 12.4822	P60	i'	38.70	30.0×5	19.7 ± 0.16
June 13.2392	P60	i'	56.86	60.0×1	>20.2
June 13.2484	P60	i'	57.08	60.0×5	>20.0
June 14.4137	P60	i'	85.05	$180. \times 1$	>18.4
June 15.2329	P60	i'	104.7	$180. \times 1$	>18.3
June 16.4076	P60	i'	132.9	$180. \times 1$	>18.8
June 17.2273	P60	i'	152.5	$180. \times 1$	>18.3
June 18.3801	P60	i'	180.2	$180. \times 1$	>18.4
June 19.3444	P60	i'	203.3	$180. \times 1$	>18.5
June 20.3703	P60	i'	228.0	$180. \times 1$	>18.4
June 20.3889	P60	i'	228.4	$180. \times 1$	>18.2

Note. — Zeropoint computed in the AB system. The UT epoch denotes the start of observations. Error quoted are 1σ photometric and instrumental errors summed in quadrature. Note that the uncertainty in the zeropoint estimate (relative to USNO-B stars) dominates but is an overestimate for variability studies using relative magnitude. Upper limits quoted are 3σ . No correction has been made for the large line-of-sight extinction.